Effect of annealing temperature on surface roughness of $BaTiO_3$ thin films deposited by vacuum evaporation method

R. SENGODAN[1,*], R. BALAMURUGAN[1], S. NITHYA[1], B. CHANDRA SHEKAR[2]
[1]*Department of Physics, Kumaraguru College of Technology, Coimbatore – 641 049, Tamil Nadu, India*
[2]*Departments of Physics, Kongunadu Arts and Science College, G.N- Mills, Coimbatore – 641029, Tamil Nadu, India*

The deposition of Barium titanate ($BaTiO_3$) thin films was performed on glass substrates that were thoroughly cleaned. The process was carried out under a pressure of 10^{-5} torr using a 12A4 Hind Hivac coating unit. The thickness of the deposited films was measured using a quartz crystal thickness monitor, which allowed for precise thickness determination. X-ray diffractometry was utilized to examine and analyze the structural properties of the films. The obtained X-ray patterns indicated that the crystallinity of the films improved as the annealing temperature increased. This suggests that higher annealing temperatures promoted the formation of well-defined crystal structures within the $BaTiO_3$ thin films. The surface roughness of the films was assessed using Speckle photography, a technique that provides insights into the roughness characteristics of a surface. The results revealed that the roughness of the films decreased as the annealing temperature was raised. This implies that higher annealing temperatures led to smoother surfaces for the $BaTiO_3$ thin films.

(Received July 25, 2023; accepted April 10, 2024)

Keywords: $BaTiO_3$, XRD, Roughness

1. Introduction

$BaTiO_3$ thin films have significant potential for various applications, including electro-optical devices [1], dynamic random-access memories (DRAM), high-speed ferroelectric random-access memories (FeRAM), tunable phase shifters and filters, radar microwave devices, humidity-sensitive sensors. These films are favored due to their low leakage current density, high dielectric breakdown strength and high dielectric constant. The preparation of $BaTiO_3$ thin films involves different methodologies such as pulsed laser ablation [5], sol-gel [2,3], chemical solution deposition [4], and radiofrequency (rf) sputtering [6]. However, high-quality $BaTiO_3$ thin films can be produced by vacuum evaporation technique.

The deposition parameters, including the method employed, temperature range for annealing process, operating gas composition and its total pressure, influence the characteristics of thin films, such as crystallinity, surface morphology, orientation and surface roughness.In our work, we focused on investigating the effects of annealing temperature on the crystallinity, surface morphology, and surface roughness of $BaTiO_3$ thin films deposited via the vacuum evaporation method. It is worth noting that while many studies have explored the properties of $BaTiO_3$ thin films prepared using various methods, there is a lack of research specifically on the surface roughness of $BaTiO_3$ thin films deposited by vacuum evaporation.

Studying the annealing temperature's impact on the aforementioned properties, reveals the influence of surface roughness in the functioning of opto-electronic devices utilizing $BaTiO_3$ thin films. This research has the potential to provide valuable insights into optimizing the deposition and annealing conditions for $BaTiO_3$ thin films, further enhancing their performance in various applications.

2. Experimental details

2.1. Preparation of thin films

The $BaTiO_3$ powder is placed on a molybdenum boat, which is heated by passing a high current (200 amps) through it. The molybdenum boat is heated by utilizing a transformer that can deliver a current of 150 amperes at 20 volts. This high current causes the $BaTiO_3$ powder to evaporate and form a vapor. Before undergoing evaporation, the evaporated material ($BaTiO_3$) undergoes a thorough degassing process at a lower temperature for around 30 minutes. During this degassing process, the shutter is closed to prevent the evaporated material from reaching the substrate. The deposition of $BaTiO_3$ onto pre-cleaned glass substrates is achieved by gradually adjusting the current. This slow current variation ensures a constant rate of evaporation throughout the preparation of the film and a consistent deposition rate of 1Å/sec is maintained. The optimal distance between the substrate and the source is found to be 0.175 m, while inside the vacuum chamber, the distance between the source and the crystal is optimized at 0.21 m. These distances are critical for controlling the deposition process and achieving the desired film characteristics. Thin films of various thicknesses are deposited to study the structure and surface roughness of the films. This analysis allows for a better understanding of the film properties and their suitability for specific applications.

2.2. Measurements

A quartz crystal monitor was employed to measure the thickness of $BaTiO_3$ thin films. The structural analysis was performed using an X-ray diffractometer with filtered CuKα radiation. Surface roughness was evaluated using speckle photography, allowing for characterization of the morphology and structure of surfaces of the films. These characterization techniques provide valuable information about the thickness, crystal structure, and surface roughness of the $BaTiO_3$ thin films.

3. Result and discussion

3.1. Structural analysis

The XRD pattern depicted in Fig. 1 illustrates the deposited BaTiO3 thin films with a thickness of 165 nm. The films were subsequently annealed at temperatures of 200 ˚C and 400 ˚C for a duration of 1 hour. The XRD patterns indicate that the $BaTiO_3$ thin films are polycrystalline, meaning they are composed of multiple crystalline domains. With an increase in the annealing temperature, the XRD patterns exhibit sharper and more intense peaks. This observation indicates that the annealing process improves the crystallinity of the $BaTiO_3$ films. Increased crystallinity typically indicates improved structural ordering and better-defined crystal planes. Both the deposited and annealed $BaTiO_3$ thin films exhibit peak splitting in the XRD patterns. This splitting is an indication of the tetragonal structure of $BaTiO_3$. The peak splitting occurs due to the distortion of the crystal lattice caused by the presence of ferroelectric domains in the material.

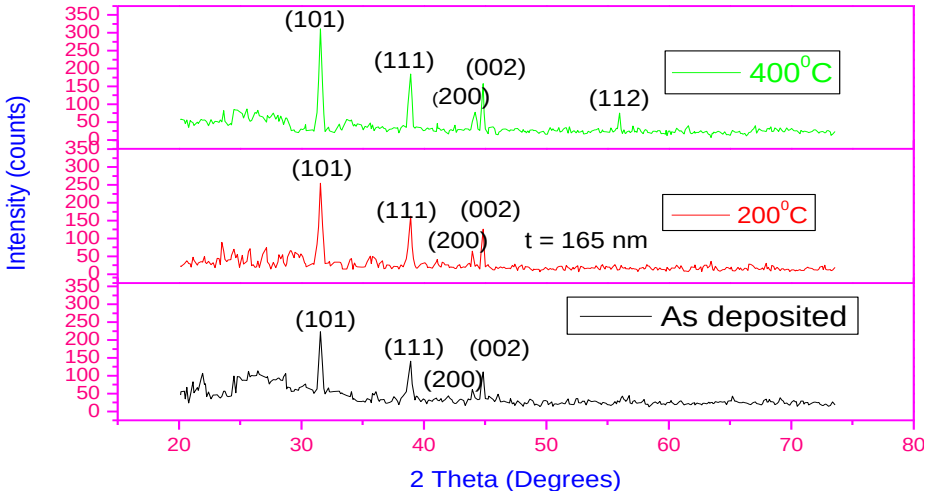

Fig.1. XRD spectrum for $BaTiO_3$ (color online)

By using the Scherrer's formula [8] the average crystallite size (D) was determined by

$$D=K\lambda/\beta\cos\theta \quad (1)$$

β – Full width half maximum of the corresponding XRD peak at radiant.
K – constant (≈0.94). θ is the Bragg's angle, λ is the wavelength of X-ray

The equation employed to estimate the dislocation density (δ) is,

$$\delta = 1/D^2 \quad (2)$$

Strain (ε) of the thin film is determined from the following formula,

$$\varepsilon = \beta\cos\theta/4 \quad (3)$$

Table 1 presents the crystallite size, strain, and dislocation density of the as-deposited $BaTiO_3$ thin film with a thickness of 165 nm, as well as the film annealed at various temperatures. The crystallite size of the as-deposited $BaTiO_3$ thin film with a thickness of 165 nm increases slightly as the annealing temperature increases. This suggests that the annealing process promotes grain growth and results in larger crystallites within the film. Larger crystallite size often indicates improved structural order and enhanced crystallinity. The strain in the $BaTiO_3$ thin films decreases as the annealing temperature increases. A decrease in strain suggests a reduction in lattice distortions or misalignments within the film. This indicates that the annealing process helps to relieve strain and improve the structural stability of the films. With an increase in the annealing temperature, there is a concurrent decrease observed in the dislocation density of the $BaTiO_3$ thin films. A decrease in dislocation density suggests a reduction in the number of crystal lattice defects, such as dislocations, within the film. Lower dislocation density is indicative of higher film quality and improved structural integrity.

Table 1. Structural parameter

Annealing temperature (˚C)	2θ (Degrees)	hkl	Crystallite size (nm)	Strain (ε) $x10^{-3}$ ($lin^{-2}m^4$)	Dislocation density (δ) $x10^{15}$ (lin/m^2)
As deposited	31.50 38.60 45.10	101 111 002	30.34 25.62 21.52	1.200 1.165 1.415	0.987 1.487 1.767
200	31.50 37.60 44.52	101 111 002	33.55 26.73 25.46	0.925 1.168 1.292	0.786 1.289 1.379
400	31.58 39.26 45.55	101 111 002	38.43 29.58 26.86	0.718 1.083 1.172	0.586 1.0123 1.124

3.2. Evaluation of surface roughness

The assessment of surface roughness on the surfaces of annealed thin films holds significant importance for engineering industries, as it directly influences the quality and characteristics of products. An experimental setup of speckle photography for $BaTiO_3$ thin film is displayed in Fig. (2). A collimated coherent He-Ne laser with a power of 1 mW and a wavelength of 532 nm, along with a CCD camera consisting of 1280 × 720 pixels, is utilized to capture speckle images of the thin film before and after annealing. To remove undesirable intensity variations resulting from ambient lighting fluctuations and other factors, pre-processing of the recorded speckle patterns is performed. When a surface is illuminated with a partially coherent laser, the observation of random bright and dark spots is referred to as speckle. The sample surface is illuminated by the He-Ne laser beam. The interference caused by scattering rays with varying optical path differences among multiple wavelets manifests as a granular intensity pattern known as speckle. The speckle contrast is quantified as the ratio between the standard deviation of the intensity and the mean of the intensity [9]. The relation between the scattered light and the surface roughness has been studied by vector diffraction and Bechmann scalar theory [10].

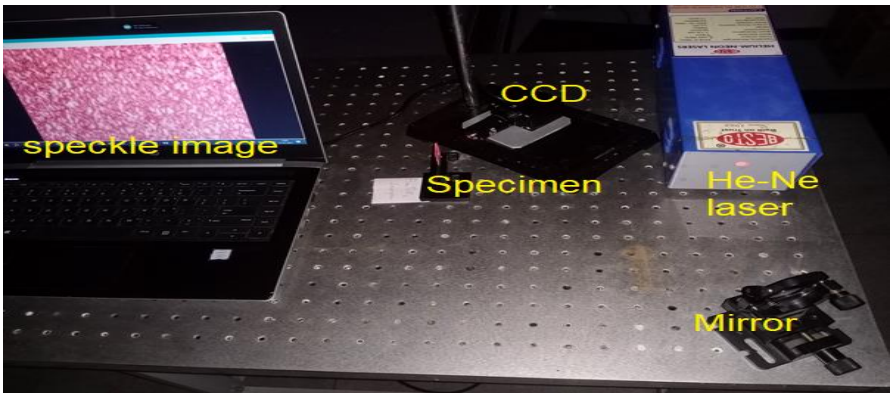

Fig. 2. Speckle photography setup for roughness estimation of $BaTO_3$ thin film (color online)

In this work, surface roughness measurement using a coherent speckle scattering pattern by a laser beam on the $BaTio_3$ thin film has been evaluated before and after annealing at 400 ˚C for 1hr. Fig. 3 shows the speckle images taken before the annealing process which means at the time of $BaTiO_3$ thin film deposition. The roughness values of the top and bottom layer line sampling values of the speckle images are shown in Fig. 3.1 and Fig. 3.2, correspondingly. In the seven-point scale of roughness, we also consider the average roughness Ra from the Left and right portion of the layer lines shown in Fig. 3.3 and Fig. 3.4 respectively. The pixel values indicate the peak and valleys in terms of Ra. Then the specimen is annealed to a temperature of 400 ˚C and the speckle images are recorded carefully picturized in Fig. 4. As in a previous way, top and bottom portions of the annealed sample Ra values are obtained by profile plot shown in Fig. 4.1 and Fig. 4.2. The left and right segmentation values are profiled in Fig. 4.3 and Fig. 4.4, respectively.

Fig. 3. Speckle image of films as deposited (color online)

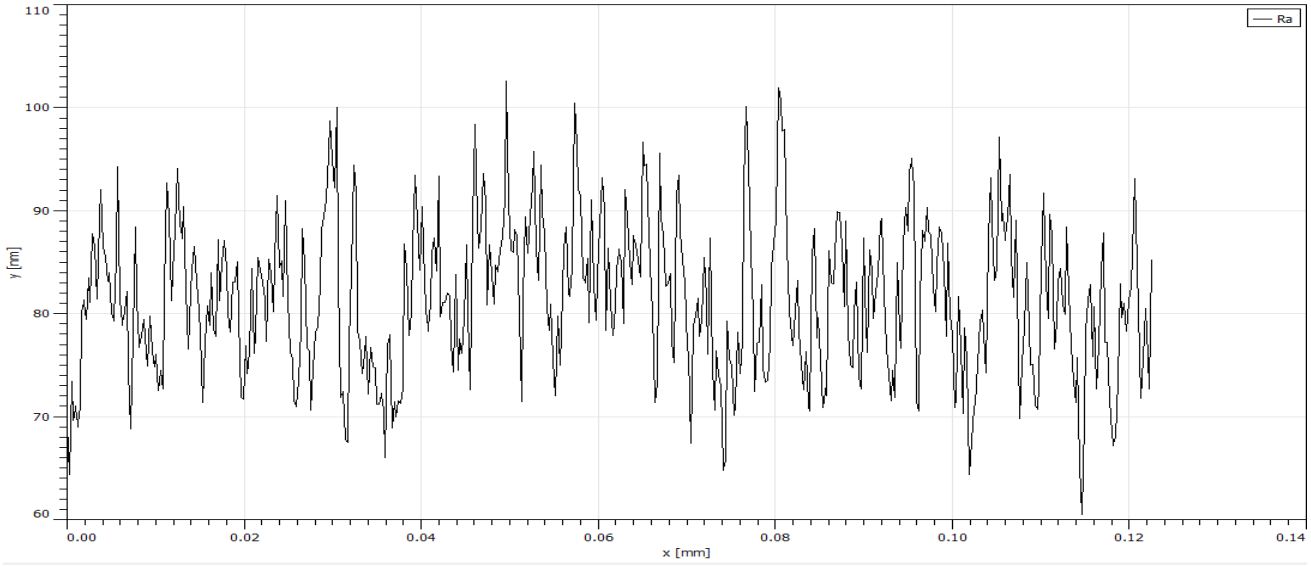

[MV1]

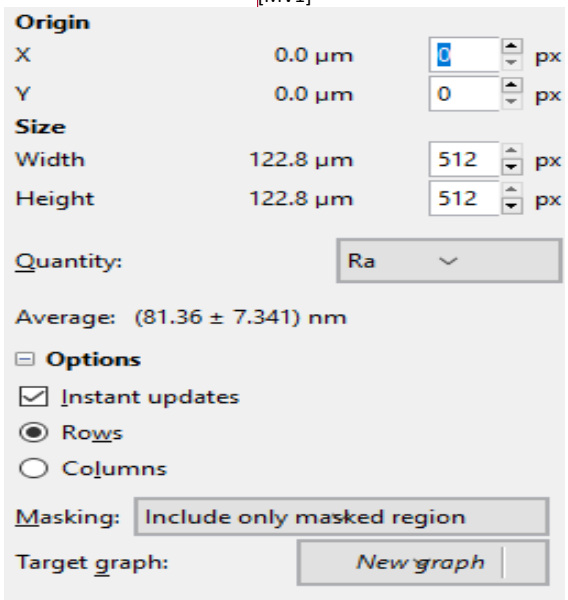

Fig. 3.1. Top portion profile of films as deposited

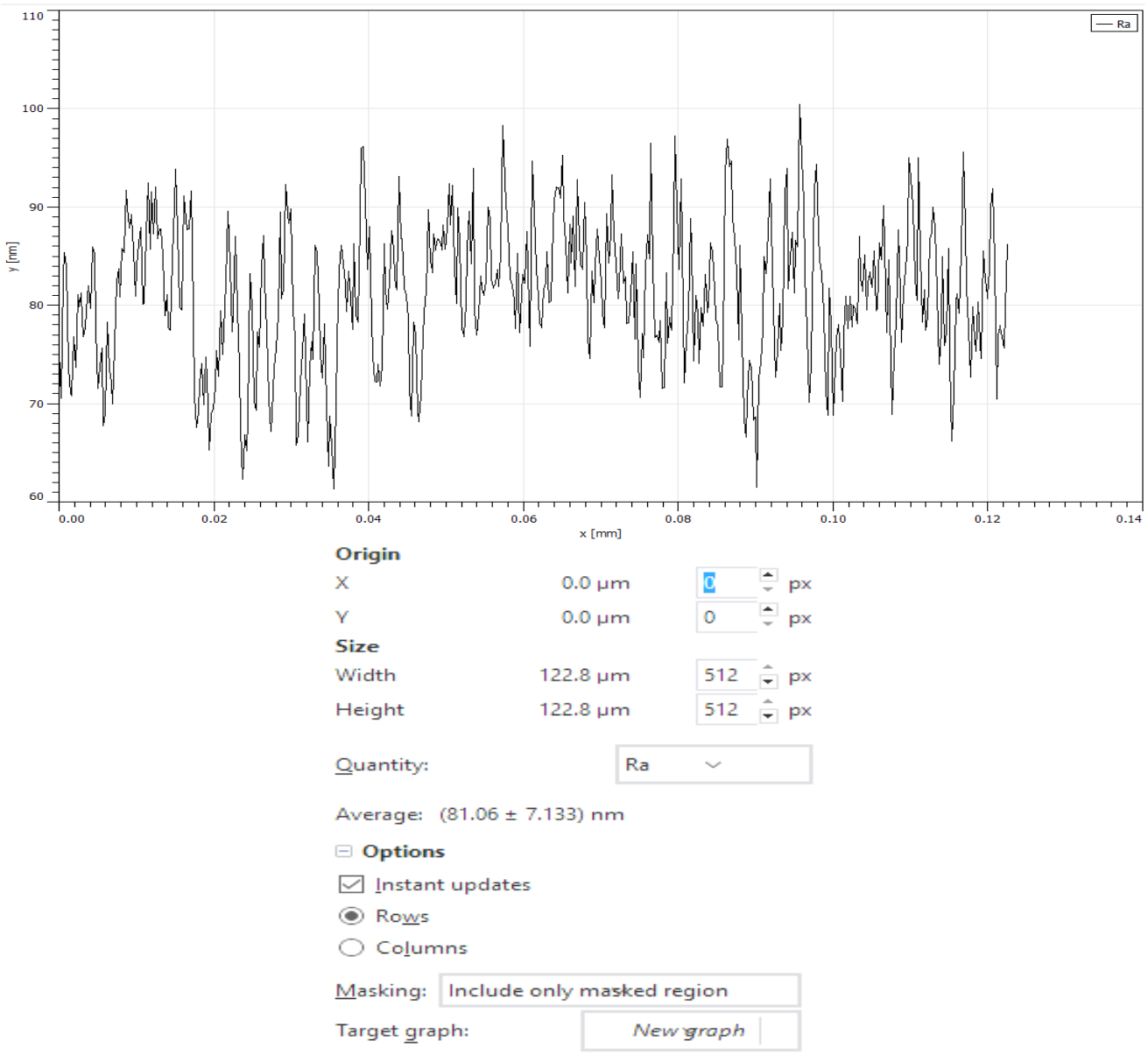

Fig. 3.2. Bottom portion profile of films as deposited

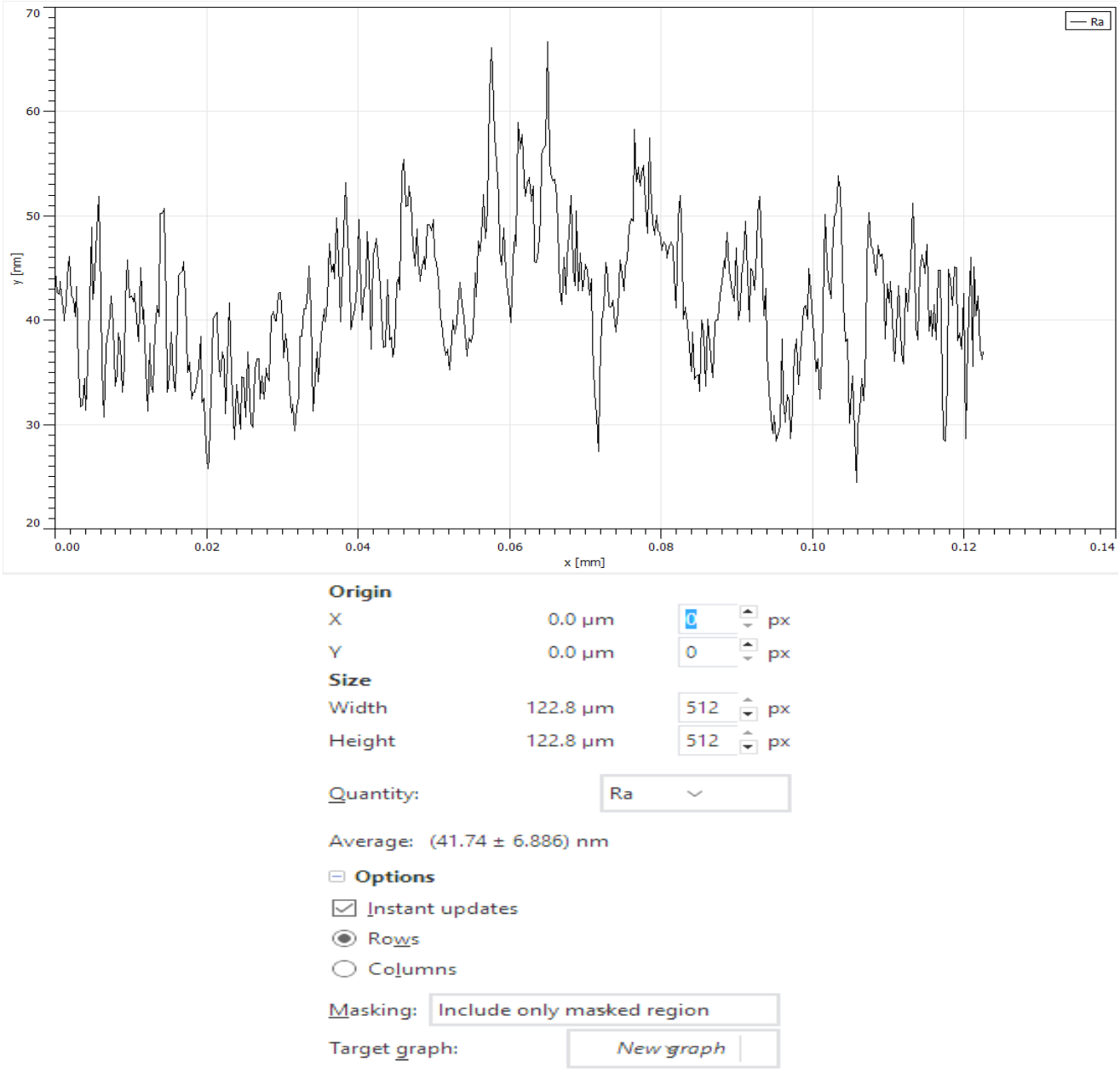

Fig. 3.3. Left portion profile of films as deposited

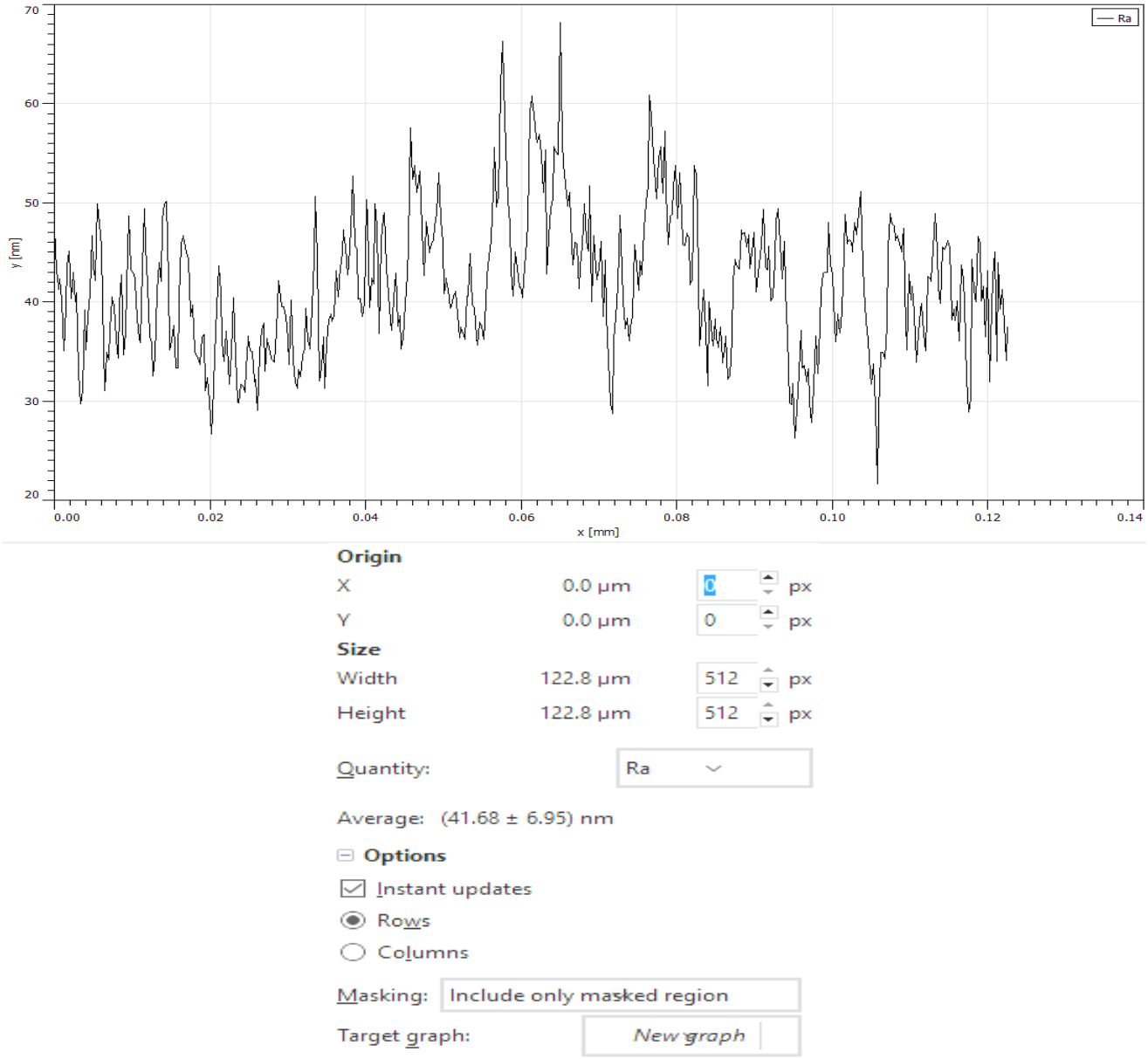

Fig.3.4. Right portion profile of films as deposited

Fig. 4. Speckle image of film annealing at 400 ˚C

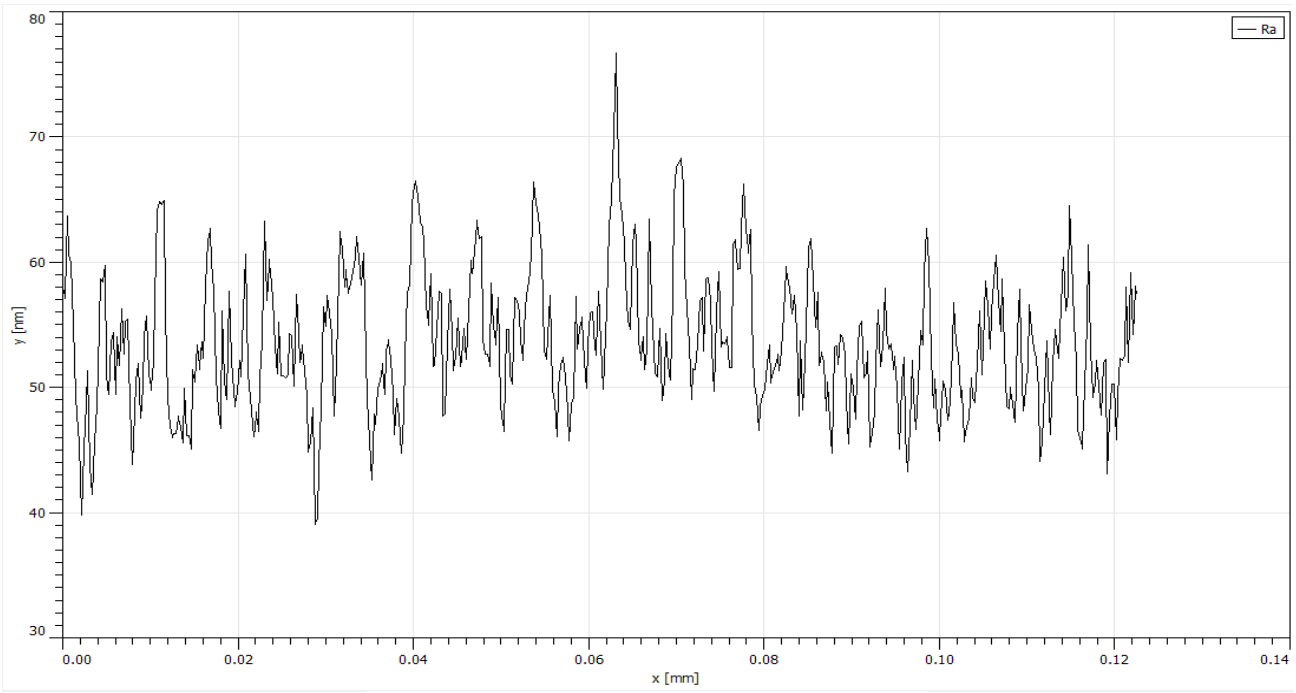

Origin

X	0.0 µm	0	px
Y	0.0 µm	0	px

Size

Width	122.8 µm	512	px
Height	122.8 µm	512	px

Quantity: Ra

Average: (53.54 ± 5.475) nm

Options

- [x] Instant updates
- (•) Rows
- ( ) Columns

Masking: Include only masked region

Target graph: New graph

Fig. 4.1. Top portion profile of film annealing at 400 ˚C

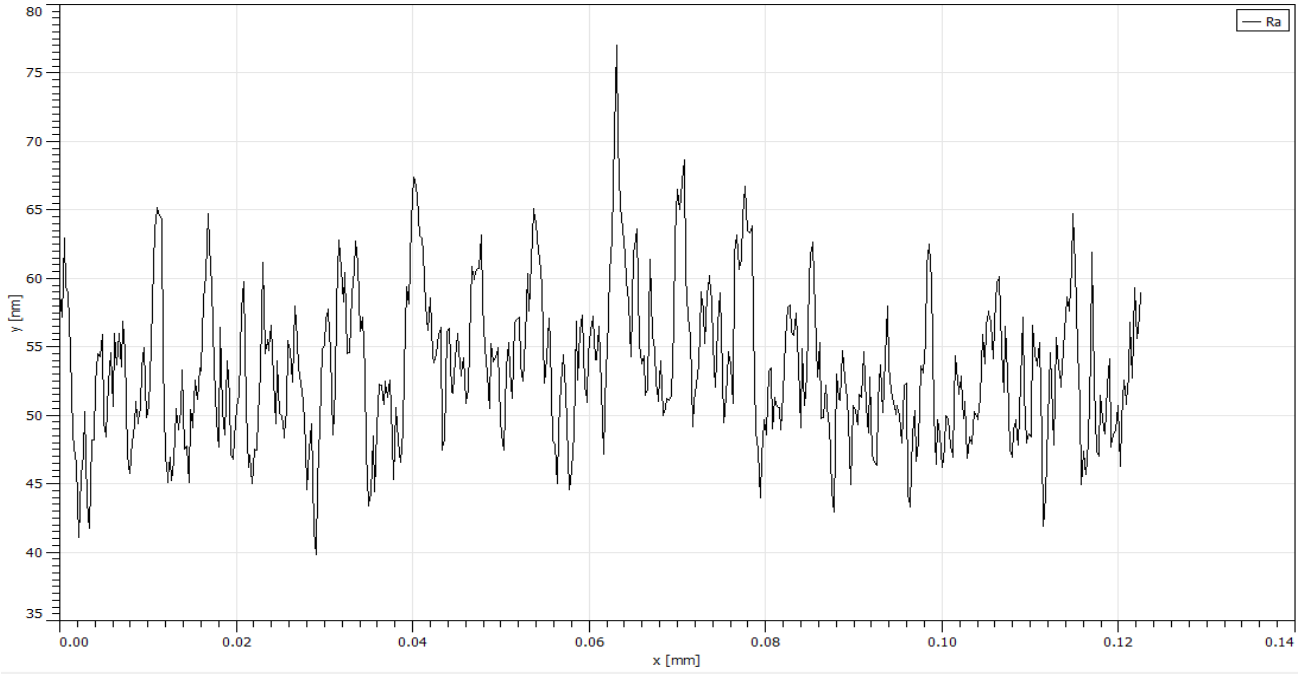

Origin

X	0.0 µm	0	px
Y	0.0 µm	0	px

Size

Width	122.8 µm	512	px
Height	122.8 µm	512	px

Quantity: Ra

Average: (53.45 ± 5.491) nm

Options

Instant updates

Rows

Columns

Masking: Include only masked region

Target graph: New graph

Fig. 4.2. Bottom portion profile of film annealing at 400 ˚C

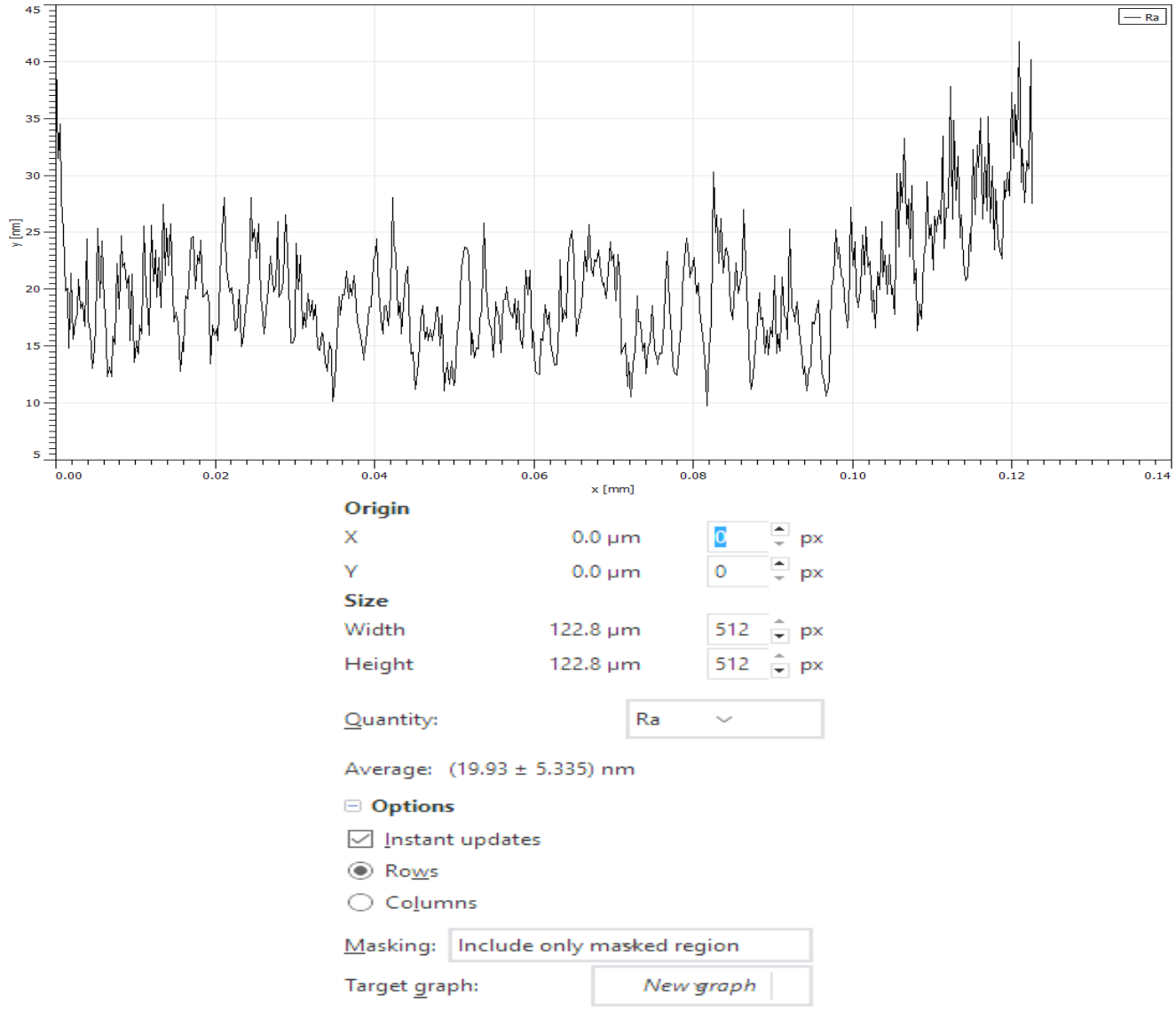

Fig. 4.3. Left portion profile of film annealing at 400 ˚C

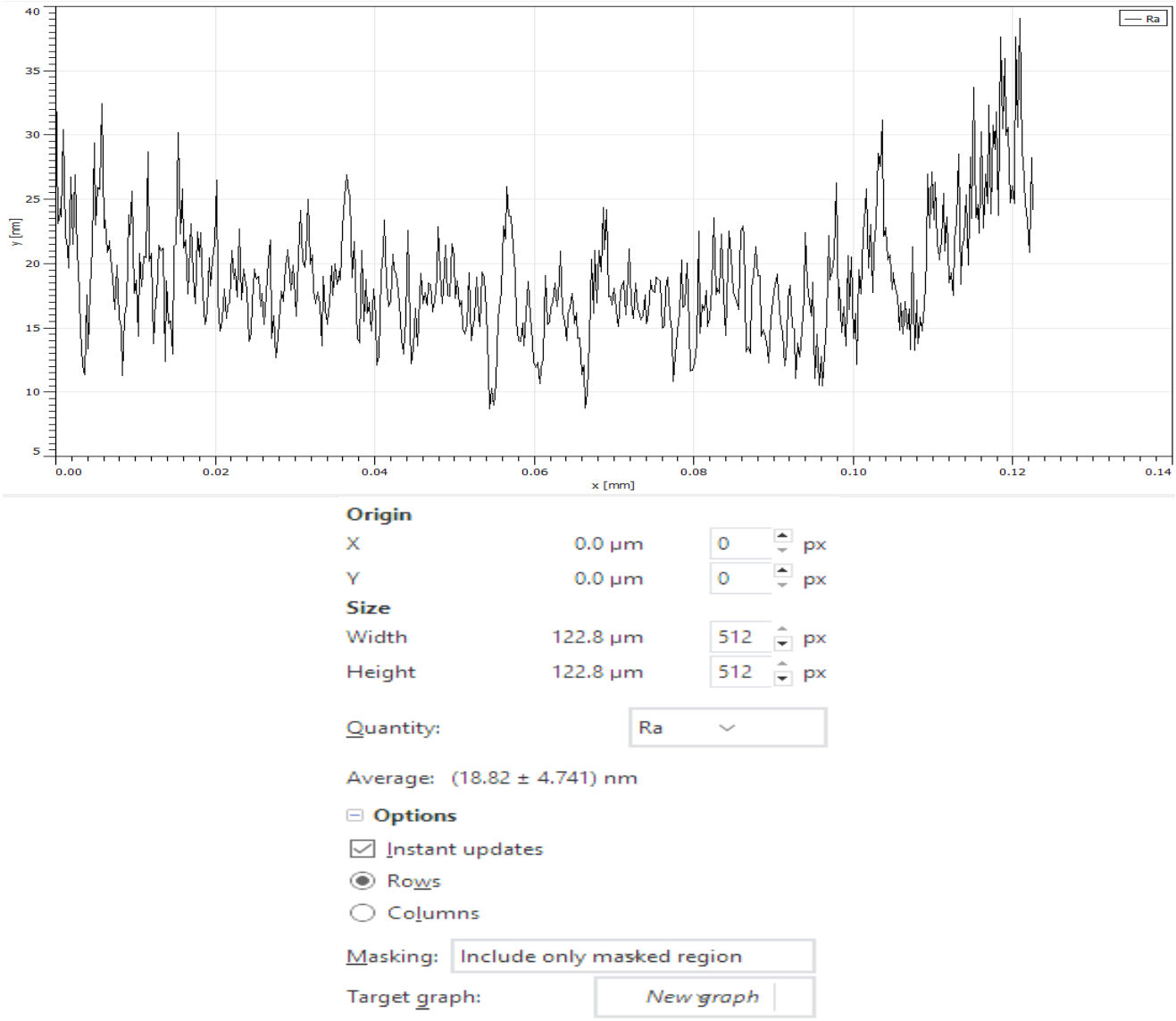

Fig. 4.4. Right portion profile of film annealing at 400 ˚C

Table 2. Roughness values before and after annealing process

S.No.	Profile places	Ra(nm) As Deposited	Ra(nm) Annealed at 400K	Roughness changes in each stage (nm)
1	Top portion	81.36	53.54	27.82
2	Bottom portion	81.06	53.45	27.61
3	Left portion	41.74	19.93	21.81
4	Right portion	41.68	18.82	22.86
5	Average value of the speckle	61.46	36.43	25.03

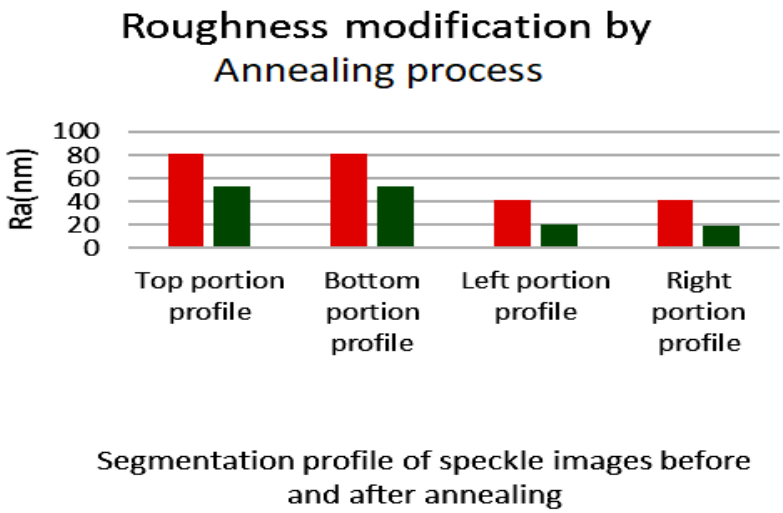

Fig. 5. Graphical representation of $BaTiO_3$ thin film before and after the annealing process color online)

The characteristics of laser speckle images help to estimate the roughness of $BaTiO_3$. This reveals that average roughness decreases with increasing the temperature of the material. It means that the annealing process makes the microstructure more crystalline. It is clear that the smoothness is enhanced. The Surface roughness of deposited $BaTiO_3$ thin films of thickness 165 nm has been evaluated before and after annealing at 400 ˚C for 1h. It is found that roughness before annealing is 61.83nm and after annealing is 36.43nm depicted in Table-1. From Graph-1, it is understood that the decrease in roughness at 25.03nm shows that increase in the crystallinity of the $BaTiO_3$ film with the rise in annealing temperature.

4. Conclusions

The deposition of barium titanate thin films on glass substrates at low pressure, followed by annealing at higher temperatures, led to an improvement in the crystallinity of the films. Additionally, the surface roughness of the films decreased as the annealing temperature was increased. These findings suggest that the annealing process positively affected the structural properties and surface quality of the thin films.

References

[1] Y. K. Vayunandana Reddy, D. Mergel, S. Reuter, V. Buck, M. Sulkowski, Journal of Physics D: Applied Physics **39**, 1161(2006).
[2] P. Bhattacharya, T. Komeda, D. Park, Y. Nishioka, J. Appl. Phys. **32**, 4103 (1993).
[3] H. B. Sharma, A. Mansingh, J. Phys. D: Appl. Phys. **31**(1), 527 (1998).
[4] Z. Hu, G. Wang, Z. Huang, X. Meng, J. Chu, Semicond. Sci. Technol. **18**, 449 (2003).
[5] J. Petzelt, T. Ostapchuk, A. Paskin, I. Rychetsky, J. Eur. Ceram. Soc. **23**, 2627 (2003).
[6] Q. X. Jia, J. L. Smith, L. H. Chang, W. A. Anderson, Phil. Mag. B. **77**, 163 (1998).
[7] J. Zhang, D. Cui, H. Lu, Z. Chen, Y. Zhou, L. Li, Japan. J. Appl. Phys. 36, 276 (1997).
[8] R. Sengodan, B. Chandra Shekar, J. Optoelectron. Adv. M. **22**(5-6), 280 (2020).
[9] A. R. Arul, H. B. Ramalingam, R. Balamurugan, R. Venckatesh, Materials Today Proceedings **92**(2), 1381 (2023).
[10] J. M. Elson, J. M. Bennett, J. Opt. Eng. **18**, 116 (1979).

*Corresponding author: Sengodan78@gmail.com